

A simple model for the calculation of the axial load-carrying capacity of corroded RC columns

G. Campione · F. Cannella · G. Minafò

Received: 13 January 2015 / Accepted: 27 April 2015
© RILEM 2015

Abstract In the present paper, a simplified model is used to determine the axial load-carrying capacity of compressed short reinforced concrete columns subjected to corrosion processes. The model considers members with circular and square cross-sections and accounts for—cover spalling, —concrete core confinement induced by transverse steel reinforcement, —buckling of longitudinal reinforcing bars. Strength reduction in concrete cover and core due to cracking induced by rust formation, reduction of steel area in longitudinal bars and transverse stirrups due to general and pitting corrosion and loss of confinement pressure are considered. The load-carrying capacity and load-axial strain curves here generated analytically fit well the existing experimental data.

Keywords Confinement · Corrosion · Buckling · Compression

1 Introduction

Corrosion of reinforcing steel is one of the main causes of deterioration of reinforced concrete (RC) structures [7, 11]. It is generally accepted that corrosion of

reinforcement affects RC structures by reducing the cross-sectional area and the mechanical properties of the reinforcement itself, especially when pitting corrosion occurs. The volume of corrosion is larger than the volume of steel lost, and the expansive products generate tensile stresses in the concrete surrounding the steel bar, which may cause cracking and spalling of concrete, and consequently a reduction of bond between concrete and reinforcement can be expected. Loss of bond between the steel and concrete, and reduction in the cross-sectional area of the reinforcement, cause a reduction in the strength and stiffness of RC members.

A typical severe damage state of corroded column is the one shown in Fig. 1. Cover spalling, buckling of steel bars, reduction of steel area due rust formation are the most visible effects.

Although the damage effects on concrete columns due to steel corrosion are well known, experimental works on the mechanical behaviour and load capacity of corroded RC columns are quite limited.

Experimental works [9, 10] have been carried out in an attempt to understand the behaviour and bearing capacity of corroded RC columns. Analytical and numerical models have also been developed and calibrated with the experimental results to predict the bearing capacity of corroded RC columns [1].

In this paper a simple model is proposed to calculate the axial load-carrying capacity of corroded columns, introducing the main parameters due to corrosion processes (reduction of steel area, concrete

G. Campione (✉) · F. Cannella · G. Minafò
DICAM, University of Palermo, Viale delle Scienze,
90128 Palermo, Italy
e-mail: studioingcampione@libero.it



Fig. 1 State of severely damaged corroded column

strength reduction). The expressions derived here allow easy hand computation and give good agreement with the experimental data available; and the model could be considered a useful tool for preliminary verification of safety in deteriorated structures. Moreover, the cases examined here do not consider the initial concrete strength, and the calculus of the load-carrying capacity is mainly intended to stress the safety factor loss reducing the distance between the design load at the ultimate state and the load-carrying capacity.

1.1 Mechanical and geometrical properties of degraded materials

The main effects on the geometrical and mechanical properties of steel and concrete during corrosion process are—reduction in the effective strength of the concrete within the cover zone, —distributed reduction of the steel area in the longitudinal bars and in the stirrups due to general corrosion, —reduction of the steel area and available ductility due to pitting corrosion.

Cracking induced by the expansion of corroded longitudinal and transverse steel bars (rust effect) degrades the strength of compressed concrete. This decrease can be related to the cracking induced by

corrosion processes (rust deposits). This reduction affects both the compressive strength of the concrete cover f'_c and of the portion of confined core f_{cc} involved in the expansion of steel bars due to rust formation.

This crack width can be expressed, as in Coronelli and Gambarova [4], by Eq. 1:

$$w_{cr} = 2 \cdot \pi \cdot (v_{rs} - 1) \cdot X \quad (1)$$

In Eq. (1) v_{rs} is taken equal to 2, as in Coronelli and Gambarova [4], and $2 \times$ is the reduction in bar diameter due to corrosion, which can be measured with the gravimetric method or calculated as suggested in Val [13] by Eq. 2:

$$X = 0.0116 \cdot i_{corr} \cdot t \quad (2)$$

where i_{corr} is the corrosion current density in the reinforcing bar expressed in $\mu A/cm^2$ and t the time in years.

The lateral strain ε_t , which causes longitudinal micro-cracks and reduces the compressive strength, can be expressed, as in Coronelli and Gambarova [4] as:

$$\varepsilon_t = \frac{b_f - b_0}{b_0} = \frac{n_{bars} \cdot w_{cr}}{b_0} = \frac{2 \cdot \pi \cdot n_{bars} \cdot (2 \cdot X)}{b_0} \quad (3)$$

with b_0 the section width without corrosion cracks, b_f the section width with corrosion cracks and n_{bars} the number of bars for side.

The reduced compressive strength can be related to ε_t , as suggested in Vecchio and Collins [14], by means of the equation:

$$\psi = \frac{f_c^*}{f_c} = \frac{1}{1 + k \cdot \frac{\varepsilon_t}{\varepsilon_0}} \quad (4)$$

with $k = 0.1$ as suggested in Coronelli and Gambarova [4], and ε_0 assumed 0.002 for normal strength, normal weight concrete.

Equation (4) is also utilized for confined concrete close to the bars replacing f_c with f_{cc} , the latter being the compressive strength of the confined concrete.

Assuming uniform distribution of corrosion around the circumference, the residual area (longitudinal bars or stirrups), according to Val [13], can be determined as:

$$A_s(t) = n \cdot \frac{\pi \cdot [\phi_0 - 2 \cdot X]^2}{4} \quad (5)$$

According to Val [13], the area reduction in steel bars due to pitting depends on chloride or carbonation-induced corrosion and chlorides may cause localized reductions of the sections. The depth of a pit, $p(t)$, which is equivalent to the maximum penetration of pitting t years after corrosion initiation, can be evaluated as:

$$p(t) = 0.0116 \cdot i_{\text{corr}} \cdot t \cdot R \quad (6)$$

According to Val [13] $R = p_{\text{max}}(t)/p_{\text{av}}(t)$ values are between 4 and 10 for 5 and 10 mm reinforcing bars of length 150–300 mm. In order to estimate the loss of a cross-sectional area of a reinforcing bar due to pitting, the model of Val [13] was utilized (as shown in Fig. 2). Based on this model, the cross-sectional area of a pit A_p , in a reinforcing bar can be calculated as:

$$A_p(t) = \begin{cases} \frac{\pi \cdot \phi_0^2}{4} - A_1 + A_2 A_p(t) \\ \frac{\pi \cdot \phi_0^2}{4} \\ p(t) \leq \frac{\phi_0}{\sqrt{2}} \\ \frac{\phi_0}{\sqrt{2}} \leq p(t) \leq \phi_0 \\ p(t) \geq \phi_0 \end{cases} \quad (7)$$

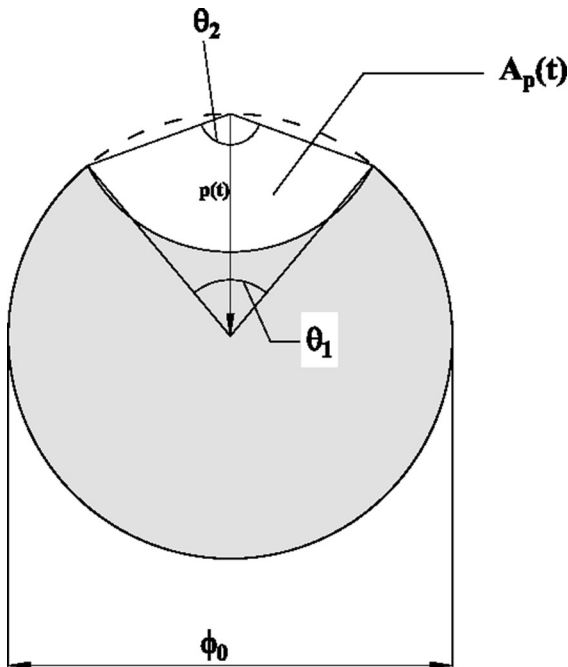


Fig. 2 Pitting model from Val [13]

$$A_1 = \frac{1}{2} \cdot \left[2 \cdot \arcsin \left(\frac{2 \cdot p(t) \cdot \sqrt{1 - \left(\frac{p(t)}{\phi_0}\right)^2}}{\phi_0} \right) \cdot \left(\frac{\phi_0}{2}\right)^2 - 2 \cdot p(t) \cdot \sqrt{1 - \left(\frac{p(t)}{\phi_0}\right)^2} \cdot \left[\frac{\phi_0}{2} - \frac{p(t)^2}{\phi_0}\right] \right] \quad (8)$$

$$A_2 = \frac{1}{2} \cdot \left[2 \cdot \arcsin \left(\frac{2 \cdot p(t) \cdot \sqrt{1 - \left(\frac{p(t)}{\phi_0}\right)^2}}{2 \cdot p(t)} \right) \cdot \left(\frac{\phi_0}{2}\right)^2 - 2 \cdot p(t) \cdot \sqrt{1 - \left(\frac{p(t)}{\phi_0}\right)^2} \cdot \frac{p(t)^2}{\phi_0} \right] \quad (9)$$

Therefore, the area of steel bars (or the same for stirrups if any) affected by pitting is:

$$A_s(t) = n \cdot \left(\frac{\pi \cdot \phi_0^2}{4} - A_p(t) \right) \geq 0 \quad (10)$$

The reduction in ultimate strain is expressed as:

$$\varepsilon'_{\text{su}} = \varepsilon_{\text{sy}} + (\varepsilon_{\text{su}} - \varepsilon_{\text{sy}}) \cdot \left(1 - \frac{\alpha_{\text{pit}}}{\alpha_{\text{pit}}^{\text{max}}} \right) \quad \alpha_{\text{pit}} < \alpha_{\text{pit}}^{\text{max}} \quad (11)$$

The application of Eq. (11) is therefore linked to the parameter $\alpha_{\text{pit}}^{\text{max}}$, whose evaluation is critical for describing the bar ductility. Different values of $\alpha_{\text{pit}}^{\text{max}}$ have been measured by various authors and values range from 0.5 to 0.1 [13].

Finally, in the presence of general corrosion and pitting the whole reduced area (longitudinal bars or stirrups) proves to be:

$$A_{\text{red}}(t) = n_{\text{bar}} \cdot \left\{ \frac{\pi \cdot [\phi_0 - 2 \cdot X]^2}{4} - A_p(t) \right\} \quad (12)$$

1.2 Axial load-carrying capacity of corroded columns

The cases examined here are those shown in Fig. 3. They refer to short RC members having a circular or square cross-section with diameter D or side b and reinforced with n longitudinal steel bars of diameter ϕ_1 and with area A_1 , and confined by transverse closed

steel spirals (or stirrups) with diameter ϕ_{st} and area A_{st} . Transverse steel is placed in the plane of the cross-section at clear spacing s with a cover δ .

The effects of corrosion considered below are—reduction of steel area of longitudinal and transverse reinforcements (Eq. 12), —reduction in compressive strength of concrete cover and of a portion of confined core (Fig. 3) due to cracking induced by rust formation (Eq. 4), —reduction in confinement pressure due to the rust formation (calculated below), —buckling effects on compressed bars due to reduction of area of longitudinal and transverse steel (calculated below).

Several models, e.g. [9], consider the inverse relationship between the concrete strength and the concrete cover depth to predict the time necessary for cover spalling leading to a loss of load-carrying due to area reduction, loss of confinement and buckling of longitudinal bars. Further studies will be addressed to including these effects in the model.

For confined concrete, to correlate the compressive strength f_{cc} and corresponding strain ε_{cc} with that of unconfined concrete and the effective confinement pressure f_{le} , the model of Razvi and Saatcioglu [8] is adopted through Eq. 13:

$$\frac{f_{cc}}{f_c} = 1 + 6.7 \cdot \left(\frac{f_{le}}{f_c}\right)^{-0.17} \quad (13)$$

$$\frac{\varepsilon_{cc}}{\varepsilon_0} = 1 + 5 \cdot \left[6.7 \cdot \left(\frac{f_{le}}{f_c}\right)^{-0.17} \cdot \frac{f_{le}}{f_c} \right] \quad (14)$$

with the confinement pressure f_{le} calculated as:

$$f_{le} = \left(\frac{2 \cdot A_{st} \cdot f_y}{b \cdot s}\right) \cdot \left(0.15 \sqrt{\frac{b}{s} \cdot \frac{b}{s_1} \cdot \left(\frac{2 \cdot A_{st} \cdot f_y}{b \cdot s}\right)}\right) \quad (15a)$$

for a square cross-section

$$f_{le} = \frac{2 \cdot A_{st} \cdot f_y}{d \cdot s} \cdot (\cos \alpha)^2 \quad (15b)$$

for a circular cross-section with a spiral

where A_{st} is the stirrup area, f_y the stirrup yield strength, b the width section, s the tie spacing, s_1 the spacing of laterally supported longitudinal reinforcing and d the diameter of the circular section. The use of f_y derived from the model of Mander et al. [6], which considered hoop tension developed by the transverse reinforcement at yield stress to determine the uniform lateral stress on the concrete core.

Equation (15a) allows one to take into account the discontinuities of the stirrups along the height, and of the number of longitudinal bars increasing the confinement effect.

The confinement pressures are calculated under the hypothesis verified experimentally [6, 8], that stirrups have to yield at concrete crushing. This phenomenon occurs in confined columns after the cover is spalled off under a sustained load close to the peak value.

If corrosion processes are taking place, the confinement pressure given by Eq. (15a, 15b) has to be reduced because of—the reduction in the area of transverse steel bars (Eq. 12), —the increase in the the

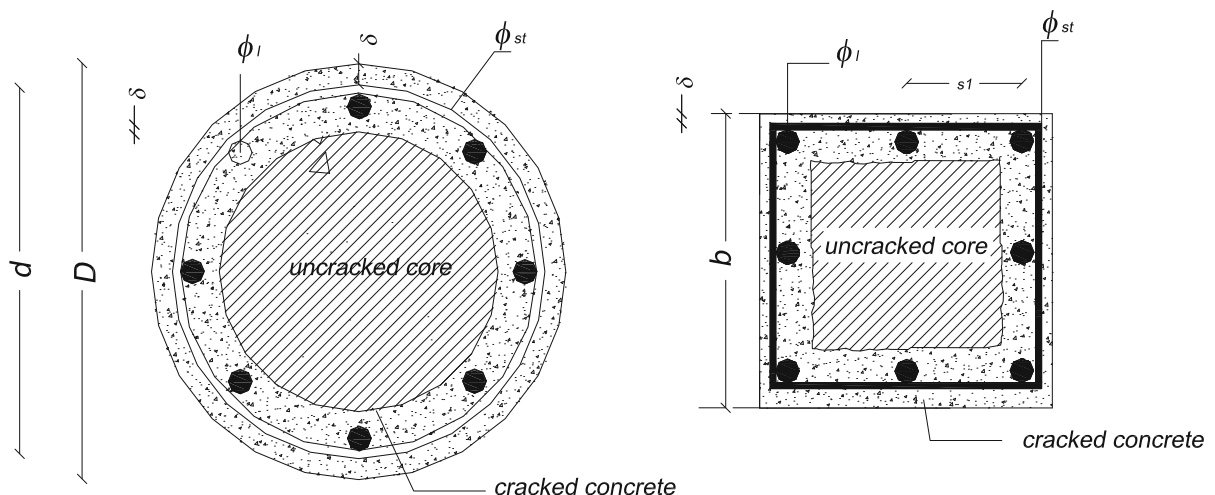


Fig. 3 Cross-sections analyzed

diameter of the longitudinal bars (rust formation) inducing concrete core cracking.

If corrosion processes are still taking place in the service condition, if the cover is spalled off due to rust formation additional tensile stress arises in the stirrup leg. Therefore this contribution has to be subtracted from the yielding stress utilized in Eq. (15a).

The free expansion of the side of the cross-section due to rust formation in the external bars is

$$\delta_y = 2 \cdot X \quad (16)$$

Consequently in the stirrup the displacement induced by rust formation determines an internal force F . This force is due to the shortening of the concrete along the side of the stirrups and to the elongation of the stirrup. If stirrup elongation alone is considered (maximum stress) we have:

$$\delta = \frac{F \cdot b}{E_s \cdot A_{st}} \quad (17)$$

Imposing compatibility of the displacements given by Eqs. 16 and 17 the value of the force F and therefore the stress in the stirrup leg is obtained in the form:

$$\sigma = \frac{2 \cdot X}{b} \cdot E_s \quad (18)$$

In Eq. (15a, 15b) the yield stress is substituted with the effective stress σ , which proves to be:

$$\sigma_s = f_y \cdot \left[1 - \frac{2 \cdot X}{b} \cdot \frac{E_s}{f_y} \right] \quad (19)$$

For longitudinal compressed bars, if the concrete cover is spalled off due to rust formation, the risk of buckling increases. Consequently, there is a dangerous reduction in the strength contribution of the main bars and in some cases also the opening of the intermediate ties occurs with some loss of confinement effects.

If the cross-section of the bar is locally reduced the ultimate strength is also reduced [2]. Hence the difference between the tensile strength of a virgin bar and that of a corroded bar is negligible, while the ultimate tensile strength is different and lower in the reduced cross-section. This is very important for plastic analysis, because the ductility of the bar is reduced.

The critical load and critical length can be calculated in a simplified manner by considering an axially loaded elastic beam on an elastic medium, which is

represented by the spread springs simulating the stirrups subjected to tensile forces. In this case in Campione and Minafò [3] the following expressions for the critical load P_{crit} and for the critical length L are obtained:

$$P_{cr} = 3.46 \cdot \sqrt{E_r \cdot I \cdot k(N)} \quad (20)$$

(or critical stress $\sigma_1 = \frac{P_{cr}}{A_t}$)

$$L = 4.77 \cdot \left(\frac{E_r \cdot J}{k} \right)^{0.25} \quad (\text{mm}) \quad (21)$$

$$E_r = \frac{4 \cdot E_s \cdot E_p}{(\sqrt{E_s} + \sqrt{E_p})^2} = E_s \cdot \frac{4 \cdot \beta}{(1 + \sqrt{\beta})^2} \quad (22)$$

with

$$I = \frac{\pi \cdot \phi_o^4}{64} \quad (23)$$

and β the share of the elastic modulus due to the hardening effect ($E_p = \beta \cdot E_s$) and k a stiffness parameter in the form [3]:

$$k = \frac{E_p \cdot A_{st}}{b} \cdot \sqrt{2} \quad \text{for a corner bar} \quad (24a)$$

$$k = \frac{48 \cdot E_p \cdot I_{st}}{s_1^3} \quad \text{for a mid-face bar} \quad (24b)$$

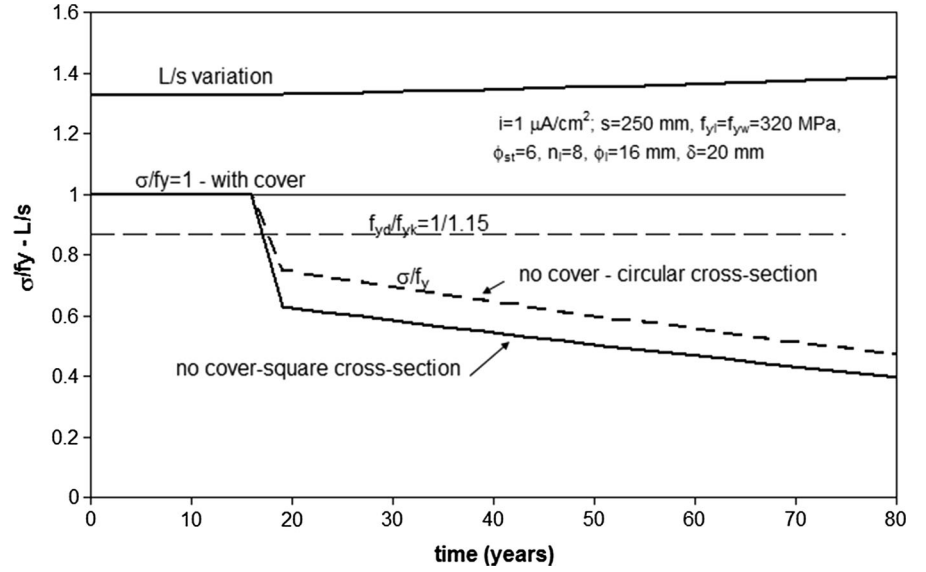
$$k = \frac{2 \cdot E_p \cdot A_{st}}{\sqrt{s^2 + d_s^2}} \quad \text{for a spiral} \quad (24c)$$

with $\beta = 1$ in the elastic range or assumed to be 0.03 at the yielding stage and $I_{st} = \frac{\pi \cdot \phi_{st}^4}{64}$, $A_{st} = \frac{\pi \cdot \phi_{st}^2}{4}$.

If we refer to the ultimate state occurring due to a high level of axial strain the cover is spalled off and the stirrups have to yield. If the corrosion process is taking place the critical length increases and the critical load decreases with the variation in time.

Figure 4 shows the reduction in critical load (dimensionless with respect to the yielding value) and the increases in the critical length L (dimensionless with respect to s) with increases in time. The examples refer to columns with—square cross-section with four corner bars and four side bars having diameter 16 mm and stirrup with diameter 6 mm at pitch 250 mm, —circular cross-section of diameter $D = b$ and having 8 ϕ 16 longitudinal bars and transverse spirals with diameter 6 mm at pitch 250 mm. The current intensity

Fig. 4 Stress reduction and critical length increases with increases in time



due to general corrosion was assumed to be $1 \mu\text{A}/\text{cm}^2$. This value represents severe corrosion conditions. It was moreover supposed that if after 20 years rust formation produced cover cracking above 1 mm the cover was ineffective and the critical stress was reduced with respect to the yielding value.

More in detail, a slight increase of the critical length was observed, while the critical stress was significantly reduced when the time increased—e.g. after 50 years the reduction was almost 35%. This aspect is very important if members are in a seismic area because the risk of buckling increases and the vulnerability of the columns also significantly increases.

The load-carrying capacity of corroded RC columns is determined as the sum of the four different strength contributions shown in Fig. 5. These terms are constituted by— P_{cover} due to the concrete cover area cracked in a biaxial state of stresses, — $P_{\text{crackedcore}}$ due to the concrete core area across the bars which are in a cracked triaxial stress state, — P_{core} due to the internal area of the concrete core which is in a triaxial stress state—and P_{sl} due to the longitudinal bars including buckling phenomena.

Considering the previous contributions one obtains:

$$P_u = \psi \cdot f'_c \cdot A_{\text{cover}} + \psi \cdot f_{cc} \cdot A_{\text{crackedcore}} + f_{cc} \cdot A_{\text{core}} + A_1 \cdot \sigma_s \quad (25)$$

with

$$A_{\text{cover}} = 4 \cdot b \cdot \delta - 2\delta^2 \quad (26a)$$

$$A_{\text{core}} = (b - 2 \cdot \delta - 2 \cdot \varphi_{\text{st}} - 2 \cdot \varphi_1)^2 \quad (26b)$$

$$A_{\text{crackedcore}} = b^2 - (4 \cdot b \cdot \delta - 2\delta^2) - (b - 2 \cdot \delta - 2 \cdot \varphi_{\text{st}} - 2 \cdot \varphi_1)^2 \quad (26c)$$

and σ_s the minimum between buckling and yielding stress.

Numerical examples in terms of dimensionless load-carrying capacity versus time increases are shown in Fig. 6 for the same data as in Fig. 4 and for two different values of current intensity (0.1 and $1.0 \mu\text{A}/\text{cm}^2$). In the same graph the ratio between design strength value f_{cd} and characteristic value f_{ck} equal to 1/1.5 (with safety factor 1.5 given by several European codes) is also given. The variations in the stress in the stirrups (σ_s/f_{yw}) and in the longitudinal bars (σ_1/f_{y1}) are also given.

The results obtained show that, without corrosion processes and in the absence of cover, the increases in the compressive strength due to confinement and the presence of unbuckled longitudinal bars ensures that the whole load-carrying capacity of the cross-section is developed; by contrast, under a severe corrosion process (simulated with a current intensity of $1 \mu\text{A}/\text{cm}^2$) the reduction in load-carrying capacity with buckled bars after 50 years is almost 20%. If pitting corrosion is also considered the strength reduction is almost the same because, seeing the low geometrical

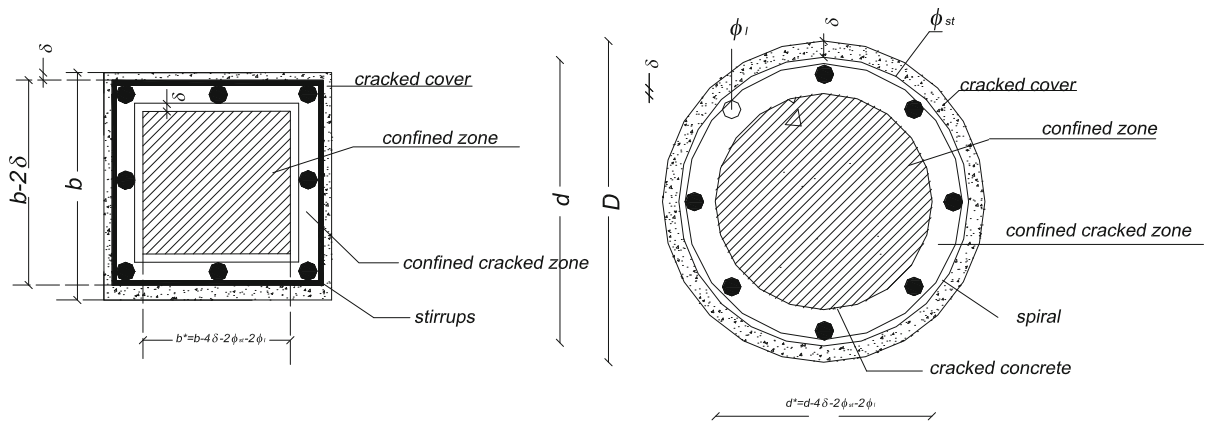


Fig. 5 Simplified model for calculus of load-carrying capacity

ratio of the steel bars adopted, the load-carrying capacity mainly depends on the load-carrying capacity of the core.

Moreover, the stress in the stirrups and longitudinal bars is strongly influenced by corrosion processes. For severe conditions, after 40 years the working stress in the stirrups approaches zero, with loss of confinement, and in longitudinal bars only 35 % of the yield stress is available.

Figure 7 shows for the same data as in Fig. 6 the variation in the load-carrying capacity for members with square and circular cross-sections, showing the major reduction that occurs in a square cross-section because of the shape of the section, which for the same diameter and stirrup pitch proves more effective in members with a circular cross-section and transverse spirals. In a static condition it has to be stressed that the risk of collapse due to the loss of bearing capacity does not occur, the ultimate load being higher than the ratio between the design strength value f_{cd} and the characteristic value f_{ck} .

1.3 Stress–strain curves for confined concrete

The stress–strain relationship adopted for unconfined concrete covers is that of Mander et al. [6] in which the coefficient ψ given by Eq. (4) is introduced to express the reduction in compressive strength due to the general corrosion, proving to be:

$$\sigma = \psi \cdot f_c \cdot \frac{\frac{\varepsilon}{\varepsilon_0} \cdot \beta}{\beta - 1 + \left(\frac{\varepsilon}{\varepsilon_0}\right)^\beta} \quad (27)$$

$$\beta = \frac{E_c}{E_c - \frac{f_c}{\varepsilon_0}} \quad (28)$$

where E_c is the initial elasticity tangent modulus of the concrete.

For confined concrete the same equations are utilized but f_c and ε_0 are replaced with f_{cc} and ε_{cc} . ψ is only applied to the cracked core, which is the area of thickness ϕ closest to the stirrups.

1.4 Stress–strain curves for longitudinal steel

The constitutive law assumed for a compressed longitudinal bar is that of Dhakal and Maekawa [5] and is given by Eq. 25 a–d:

$$\frac{\sigma}{\sigma_1} = 1 - \left(1 - \frac{\sigma^*}{\sigma_1^*}\right) \cdot \left(\frac{\varepsilon - \varepsilon_y}{\varepsilon^* - \varepsilon_y}\right) \quad \varepsilon_y < \varepsilon \leq \varepsilon^* \quad (29a)$$

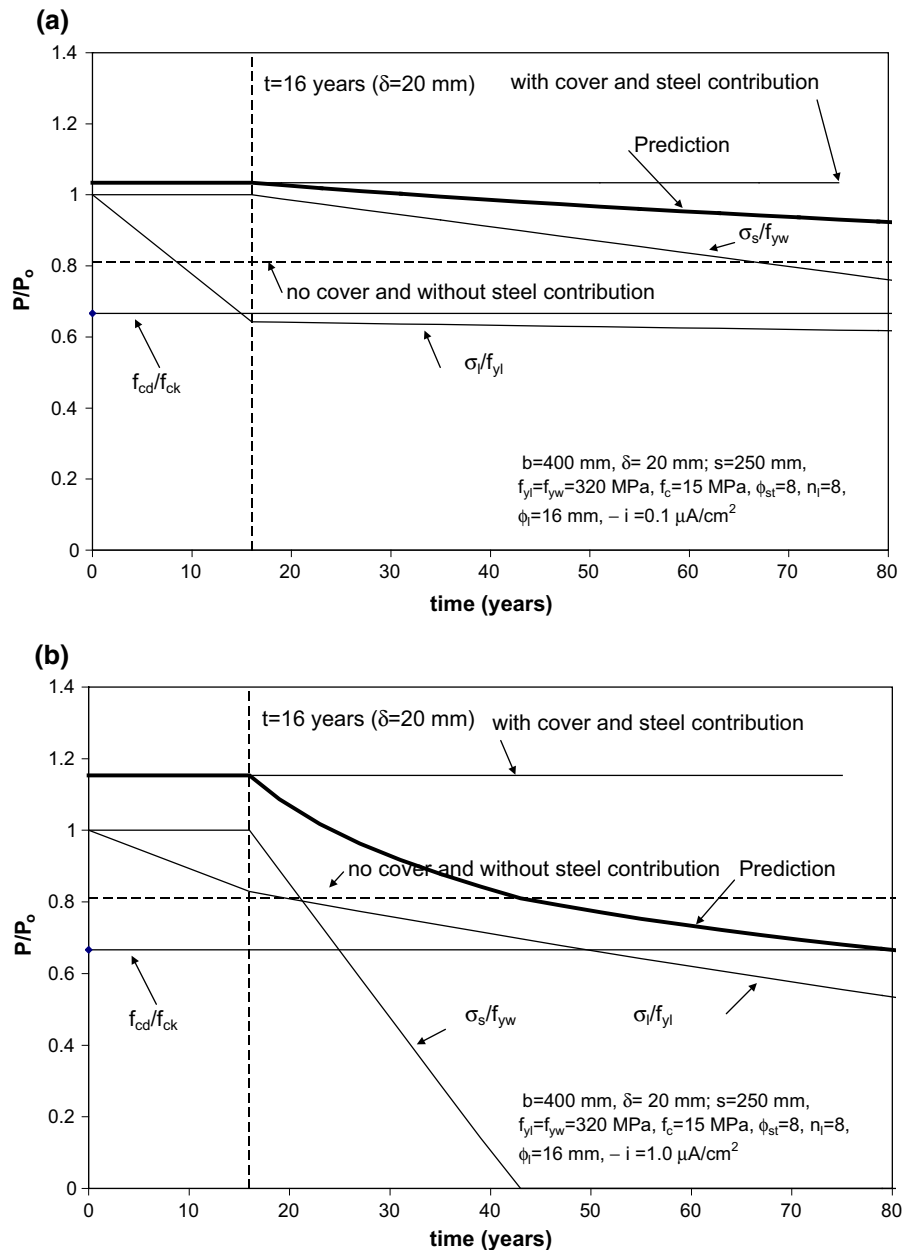
$$\sigma \geq 0.2 f_y; \quad \sigma = \sigma^* - 0.02 E_s (\varepsilon > \varepsilon^*) \quad \varepsilon > \varepsilon^* \quad (29b)$$

$$\frac{\varepsilon^*}{\varepsilon_y} = 55 - 2.3 \cdot \sqrt{\frac{f_y}{100}} \cdot \frac{L}{\phi_1} \quad \frac{\varepsilon^*}{\varepsilon_y} \geq 7 \quad (29c)$$

$$\frac{\sigma^*}{\sigma_1^*} = \alpha \cdot \left(1.1 - 0.0116 \cdot \sqrt{\frac{f_y}{100}} \cdot \frac{L}{\phi_1}\right) \quad \frac{\sigma^*}{f_y} \geq 0.2 \quad (29d)$$

α being 1 for linear hardening bars and 0.75 for perfectly elastic–plastic bars, and L being the buckling length.

Fig. 6 Axial load-carrying capacity for members with square cross-section and different values of current intensity ($\mu\text{A}/\text{cm}^2$): **a** 0.1; **b** 1.0

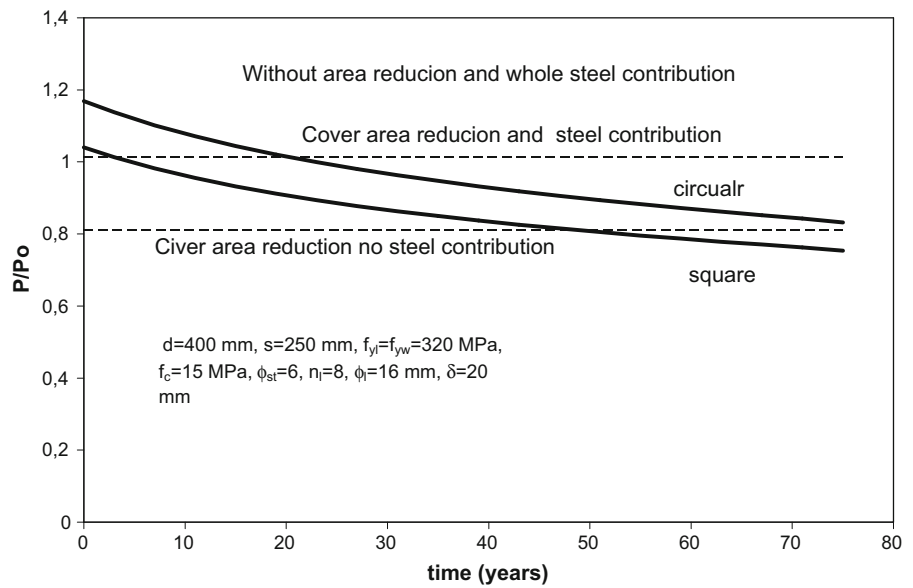


1.5 Experimental validation

In this section the suitability of the model is verified with experimental data referring to members with square and circular cross-sections. The data for columns with a square cross-sections were those of Uomoto and Misra [12] and Rodriguez et al. [9], while those for members with a circular cross-section and steel spirals are those of Bae et al. [1].

Uomoto and Misra [12] tested ten columns with a square cross-section and side 100 mm and length 400 mm. The longitudinal reinforcement was constituted by four 10-mm deformed bars, one in each corner, with a 20-mm cover. The stirrups, constituted by deformed bar, had a diameter of 6 mm and the stirrup pitch was 75 mm. Two levels of sodium chloride (1.0 and 6.6 kg/m^3) were added to the mix water. Two corrosion currents were applied (45 and

Fig. 7 Load-carrying capacity variation with increases in time for members with square and circular cross-sections



180 mA) for either 2 or 10 days. No pre-loading was applied during the corrosion period. An axial load was applied to the columns. The failure mode of the columns was characterized by spalling of the concrete cover and buckling of the longitudinal reinforcement. The two columns with least corrosion (45 mA for two days) had residual load-carrying capacities of 88 and 98 % of the control columns (type 1 in Table 1). The other six corroded columns (180 mA and 10 days) had residual load-carrying capacities ranging from 77 to 84 % of the control (type 2 of Table 1). The reductions in load-carrying capacity were larger than could be explained on the basis of reinforcement area loss alone.

Rodriguez et al. [9] tested in compression 24 columns subjected to accelerated corrosion processes. The columns had a square cross-section with side 200 mm and length 2000 mm. The columns tested were divided into three groups. Type 1 columns were reinforced with four longitudinal bars 8 mm in diameter and stirrups 6 mm in diameter at pitch 100 mm. Type 2 columns had four 16-mm main bars and stirrups 6 mm in diameter at pitch 150 mm. Type 3 columns had eight longitudinal bars 12 mm in diameter and stirrups 6 mm in diameter at pitch 150 mm. A cover of 20 mm was adopted for all groups.

Sodium chloride (by weight of cement) in the percentage of 3 % was added to the mixing water, and

a current of 0.1 mA/cm² was applied to all the reinforcement.

For the type 1 columns, the residual load-carrying capacity ranged from 64 % of the control column at 15.4 % corrosion in the main bars to 56 % at 27.8 % corrosion (type 3 in Table 1).

The results confirmed that the loss in load-carrying capacity was far greater than could be explained by loss of steel area and cover spalling as shown in Table 1. Rodriguez et al. [9] also observed that a phenomenon of premature buckling of the corroded reinforcement occurs.

For the case mentioned before Table 1 shows a comparison between experimental and analytical values obtained with the proposed model expressed in terms of percentage of loss of load-carrying capacity. The comparison shows good agreements and specifically the application of the model allows one to verify the experimental failure mode, the latter consisting in cover spalling and buckling of longitudinal bars. The result also confirmed the hypothesis made in developing the model that a part of the confined core affected by rust formation reduced the compressive strength of the confined concrete, further aggravated by the loss of confinement induced by the reduction in the stirrup area.

Bae et al. [1] tested in compression small-scale RC columns. The diameter of the columns was 152 mm and the height was 457 mm. Deformed reinforcing

Table 1 Reduction in the load-carrying capacity of columns with square cross-sections due to corrosion

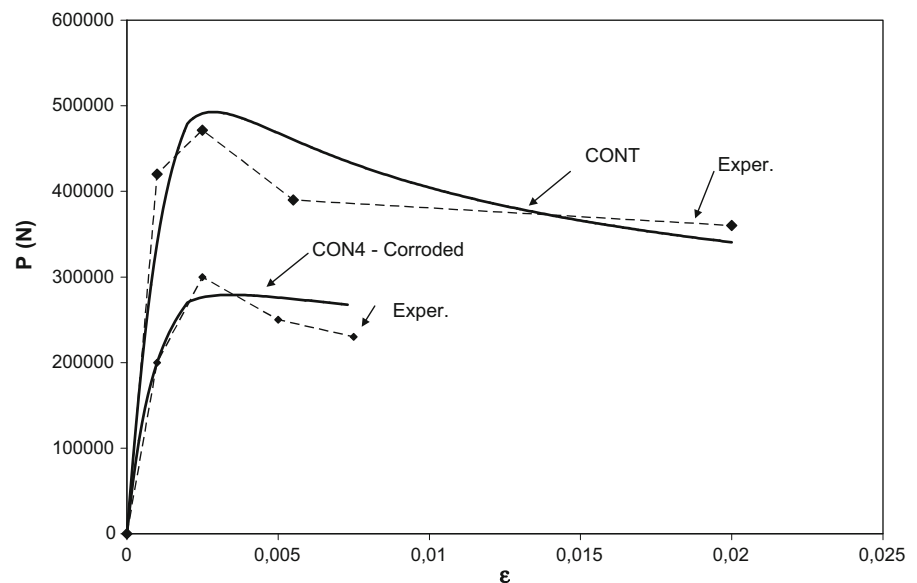
Author	Type	Experimental (%)	Analytical (%)
Uomoto and Misra [12]	1	88	86
Uomoto and Misra [12]	2	84	85
Rodriguez et al. [9]	3a	64	59
Rodriguez et al. [9]	3b	56	58
Rodriguez et al. [9]	4a	58	53
Rodriguez et al. [9]	4b	54	46
Rodriguez et al. [9]	5a	63	51
Rodriguez et al. [9]	5b	51	43
Average and standard deviation		Exp./Analy = 1.09	ST.DEV. = 0.098

bars with a diameter of 9.5 mm and yield strength of 414 MPa were used as longitudinal reinforcement. Steel wires with a diameter of 3.7 mm at pitch 25 mm were used as spiral reinforcement. The concrete strength was 21 MPa at the time of testing. The accelerated corrosion process was achieved by wet-dry cycles and imposing an electric potential between the anode and cathode reinforcement. Compressive tests were conducted for specimens without corrosion processes (denoted as CONT specimen) and on specimens after completion of the accelerated corrosion process (denoted as CON4 specimen). The tests showed that spalling of the concrete cover of the corrosion-damaged columns (CON4) occurred along the height of the columns almost at the same time,

showing the significant loss of failure load with respect to the control columns (CONT).

A comparison in terms of load-axial strain curves is shown in Figs. 7 and 8. The axial load-axial strain curves were determined with the following steps—an initial value of axial shortening ε was assumed,—the effective confinement pressure due to the transverse steel was computed,—the compressive strength of the confined concrete and corresponding strain was calculated; the strength contribution due to the concrete cover, cracked core and effectively confined core was calculated; and finally the load P was determined as the sum of the previous contributions. Repeating this procedure for all possible axial strain values the complete load-strain curve was plotted.

Fig. 8 Load-axial strain curves for specimens tested in Bae et al. [1]



2 Conclusions

In the present paper an analytical model to calculate the axial load-carrying capacity of compressed RC corroded columns was developed and verified against available experimental data. The cases examined refer to short compressed members with circular and square cross-sections. Different arrangements of longitudinal and transverse steel bars (spirals and stirrups) were examined. General and pitting corrosion were included in the model showing that they produce a reduction in load-carrying capacity.

The results obtained show that the main causes of loss of load-carrying capacity due to corrosion processes are—cover expulsion, —cracking of the portion of confined core closest to the longitudinal bars and stirrups, —reduction in the steel area. It also has to be stressed that the reduction in the load-carrying capacity due to loss of mass of longitudinal bars is not significant for compressed members under static loads, while the reduction in load-carrying capacity is between 20 and 30 % for severe corrosion conditions because the process involves mainly the outer portion of the column.

However, under actions that induce axial force and bending moment, a corrosion process produces buckling of longitudinal bars and loss of confinement due to the loss of stirrup mass, which can reduce drastically the bearing capacity and the available ductility of the column.

References

1. Bae SW, Belarbi A, Myers JJ (1999) Performance of corrosion-damaged RC columns repaired by CFRP sheets. *ACI Spec Publ SP-230* 82:1447–1464
2. Cains J, Plizzari GA, Du Y, Law D, Franzoni C (2005) Mechanical properties of corrosion-damaged reinforcement. *ACI Mater J* 102(4):256–264
3. Campione G, Minafò G (2010) Compressive behavior of short high-strength concrete columns. *Eng Struct* 32: 2755–2766
4. Coronelli D, Gambarova P (2004) Structural assessment of corroded reinforced concrete beams: modeling guidelines. *ASCE J Struct Eng* 130:1214–1224
5. Dhakal RP, Maekawa K (2002) Modeling for post-yield buckling of reinforcement. *J Struct Eng ASCE* 128(9): 1139–1147
6. Mander JB, Priestley MJN, Park R (1988) Observed stress-strain behavior of confined concrete. *J Struct Eng ASCE* 114(8):1804–1826
7. Pedferri P, Bertolini L (2000) *La durabilità del calcestruzzo armato*. McGraw-Hill, Milano (only available in Italian)
8. Razvi S, Saatcioglu M (1999) Confinement model for high-strength concrete. *J Struct Eng ASCE* 125(3):281–288
9. Rodriguez J, Ortega LM, Casal J (1996) Load-carrying capacity of concrete columns with corroded reinforcement, Fourth international symposium on the corrosion of reinforcement in concrete structures, Cambridge, UK, 1996, pp 220–223
10. Rodriguez J, Ortega LM, Casal J (1997) Load-carrying capacity of concrete structures with corroded reinforcement. *Constr Build Mater* 11(4):239–248
11. Tuutti K (1982) Corrosion of steel in concrete.” Fo 4.82, Swedish Cement and Concrete Research Institute, Stockholm, Sweden
12. Uomoto T, Misra S (1990) Behaviour of concrete beams and columns in marine environment when corrosion of reinforcing bars takes place, *Concrete in marine environments*. *ACI SP 109-6*(1990):127–146
13. Val DV (2007) Deterioration of strength of RC beams due to corrosion and its influence on beam reliability. *ASCE J Struct Eng* 133(9):197–1306
14. Vecchio F, Collins MP (1986) The modified compression field theory for reinforced concrete elements subjected to shear’. *Proc ACI* 83(2):219–231